

Supporting Information (SI)

Engineering lignin-derivable diacrylate networks with tunable architecture and mechanics

Yu-Tai Wong¹, LaShanda T. J. Korley^{1,2}*

¹Department of Chemical and Biomolecular Engineering, University of Delaware, Newark, Delaware 19716, United States

²Department of Materials Science and Engineering, University of Delaware, Newark, Delaware 19716, United States

*Corresponding author, E-mail: lkorley@udel.edu

Abbreviations

BGF	Bisguaiacol F
BGFDA	Bisguaiacol F diacrylate
BA	<i>n</i> -butyl acrylate
DCM	Dichloromethane
E_t	Young's modulus
$T_{d,5\%}$	Degradation temperature at 5 wt% loss
T_g	Glass transition temperature
VDA	Vanillyl alcohol diacrylate
ε_B	Elongation-at-break
σ_M	Ultimate tensile strength

Proton (^1H) Nuclear Magnetic Resonance (NMR) spectra for lignin-derivable building blocks in deuterated chloroform (CDCl_3)

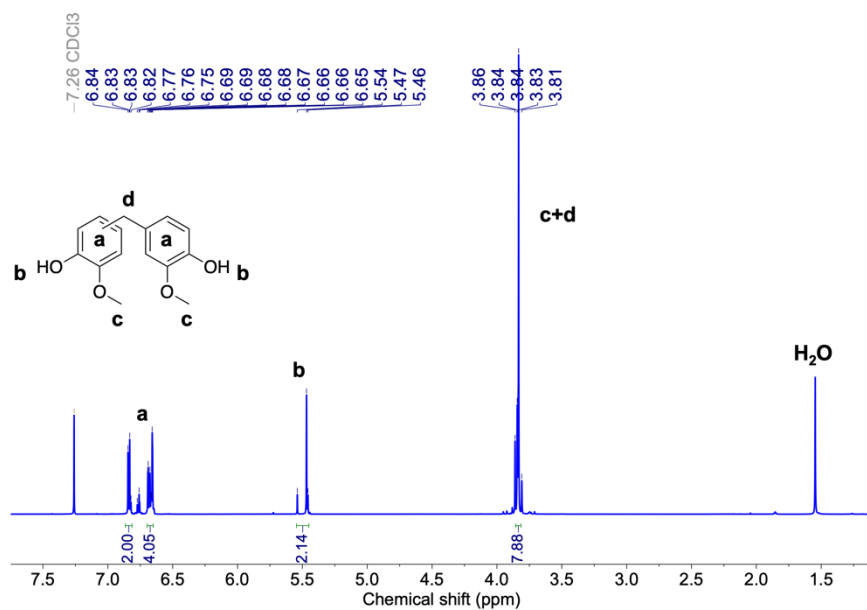


Fig. S1 ^1H NMR spectrum of bisguaiacol F

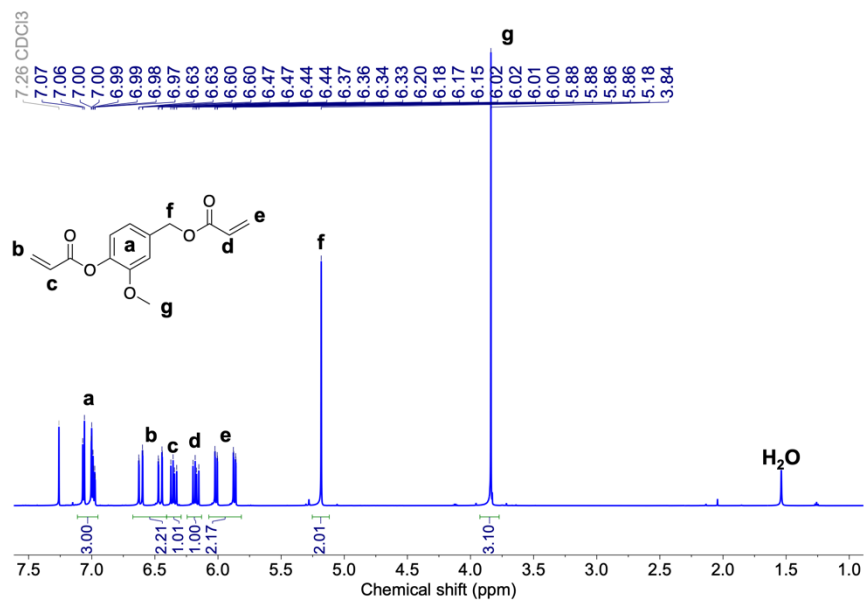


Fig. S2 ^1H NMR spectrum of vanillyl alcohol diacrylate

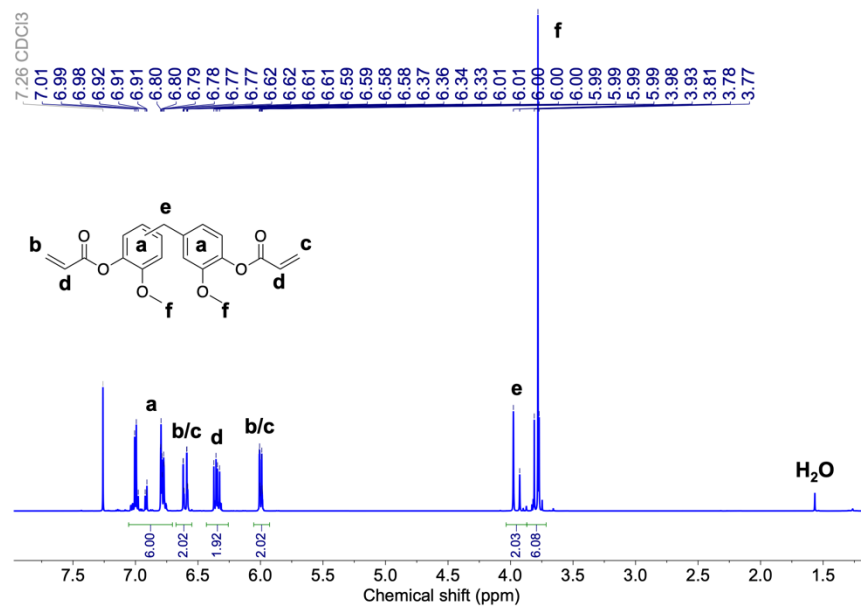


Fig. S3 ^1H NMR spectrum of bisguaiacol F diacrylate

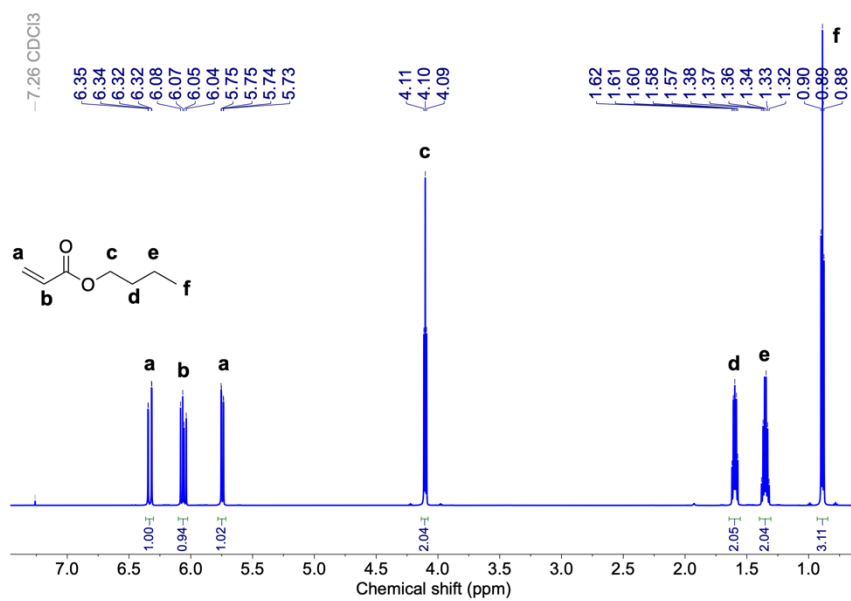


Fig. S4 ^1H NMR spectrum of *n*-butyl acrylate

Film curing steps and film appearances

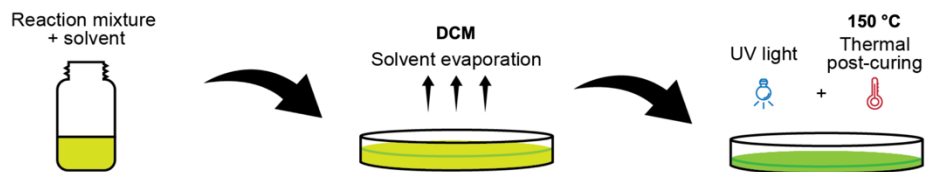


Fig. S5 Schematic representation of film casting and curing procedures



Fig. S6 Optical images of each acrylate networks after thermal post-curing with a film thickness ~ 0.2 mm

Differential scanning calorimetry (DSC) results for curing of acrylate networks

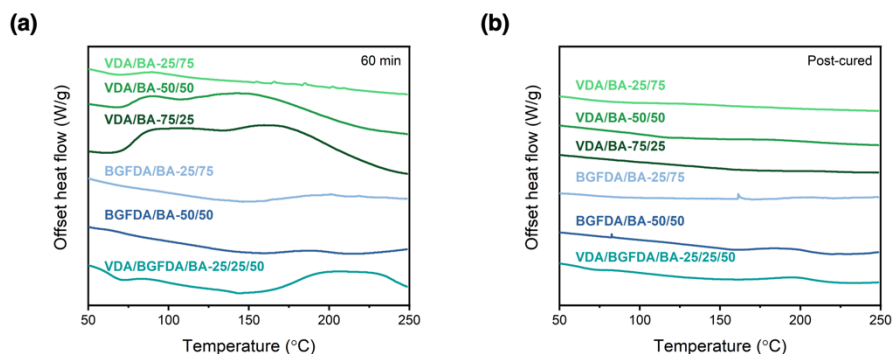


Fig. S7 DSC curve of acrylate networks (a) before and (b) after thermal post-curing (exotherm up, 10 °C/min, N₂). Exothermic peaks in (a) were applied to determine the temperature for thermal post-curing.

Attenuated total reflectance-Fourier transform infrared (ATR-FTIR) spectra for acrylate networks

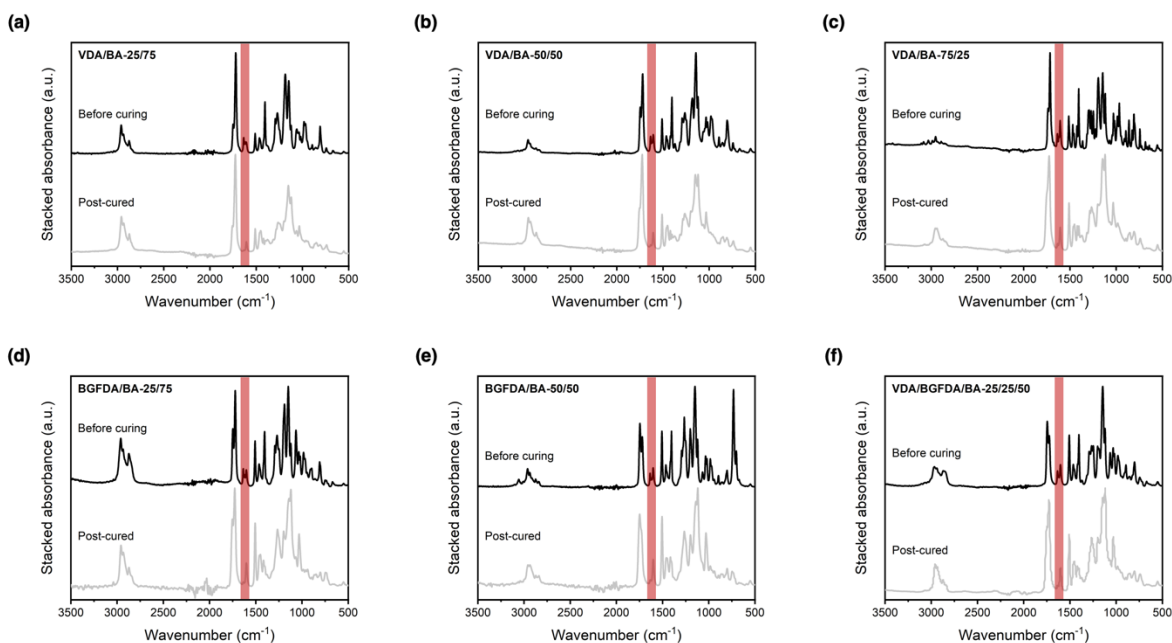


Fig. S8 Stacked ATR-FTIR spectra of acrylate networks before and after thermal post-curing. The conversion was probed quantitatively by the disappearance of the acrylate carbon double bond stretching band at ~1635 cm⁻¹ (highlighted in red) with an internal reference of carbonyl double bond stretching band at ~1724 cm⁻¹ (128 scans, resolution 4 cm⁻¹).

Thermogravimetric analysis (TGA) results of acrylate networks

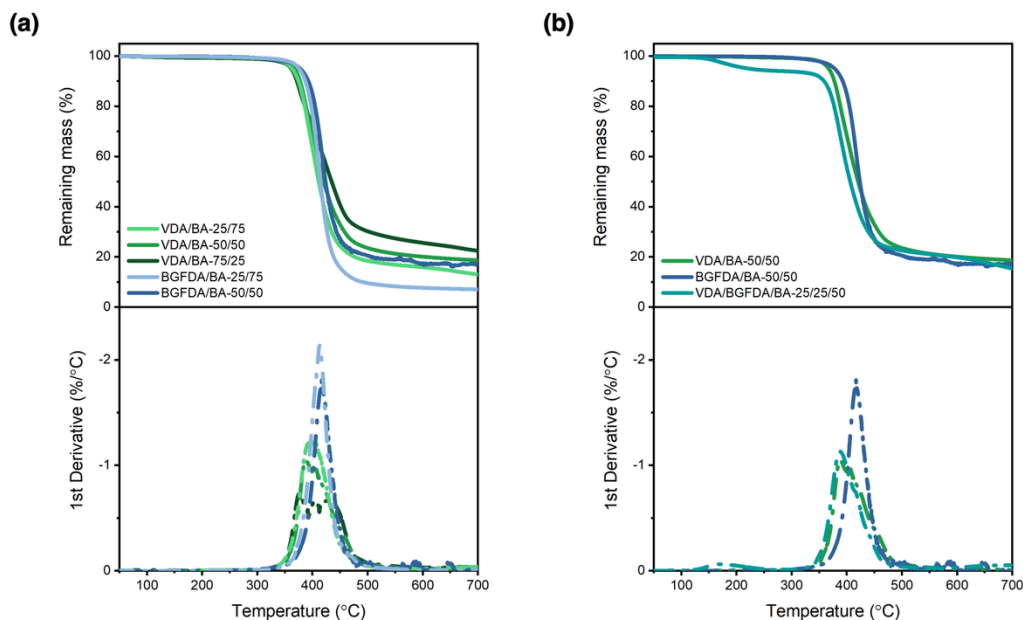


Fig. S9 Thermogravimetric analysis traces and respective first-derivative curves of acrylate networks for (a) varying diacrylate content and (b) varying diacrylates (10 °C/min, N₂).

Table S1 $T_{d,5\%}$ of acrylate networks.

Sample	$T_{d,5\%}$ (°C)
VDA/BA-25/75	363
VDA/BA-50/50	367
VDA/BA-75/25	361
BGFDA/BA-25/75	376
BGFDA/BA-50/50	378
VDA/BGFDA/BA-25/25/50	222

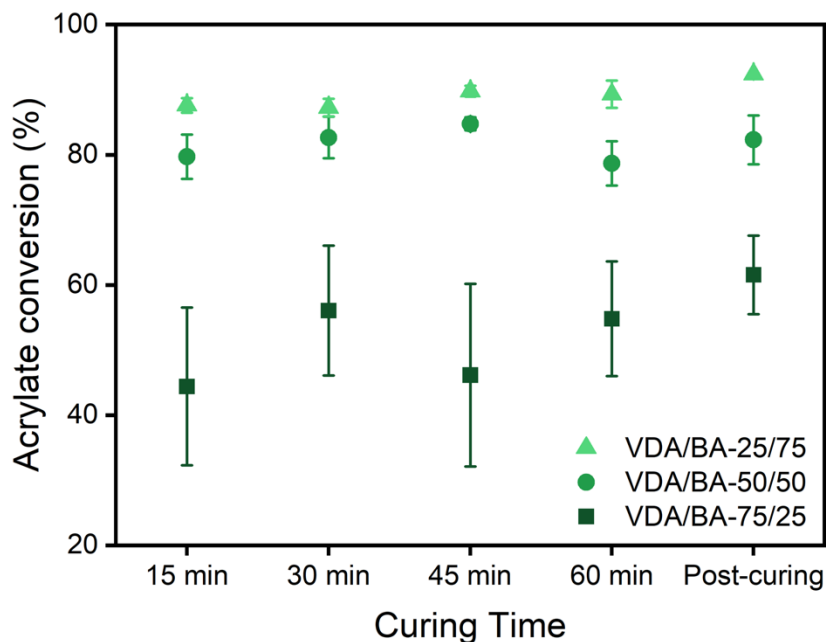


Fig. S10 Conversion profile of VDA/BA networks at different curing times as an example of the evolution of network formation. Each data point represents the triplicated result using samples from different batch.

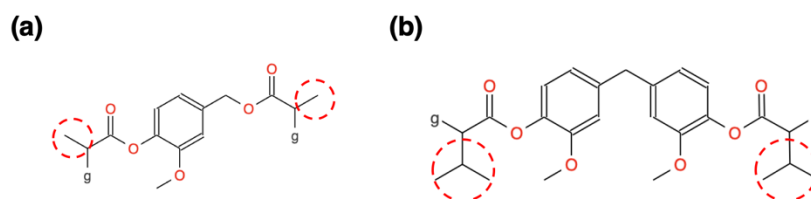


Fig. S11 Structures used to predict T_g s of the homopolymer for (a) VDA and (b) BGFDA *via* Polymer Genome. ‘g’ represents the bond with repeated units, and side groups marked with red dashed circle denote the structure added manually to mimic crosslinked structure. The predicted T_g for VDA homopolymer is 194 °C and BGFDA homopolymer is 222 °C.

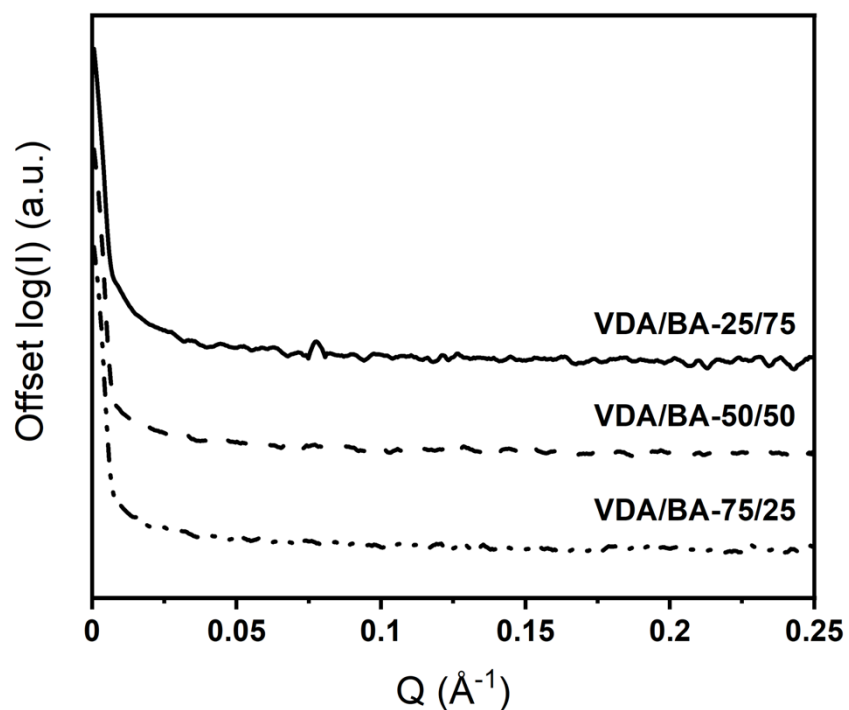


Fig. S12 Small-angle X-ray scattering spectra for VDA/BA networks. Curves are based on absolute scale and shifted vertically for clarity (sample-to-detector distance: 1200 mm).

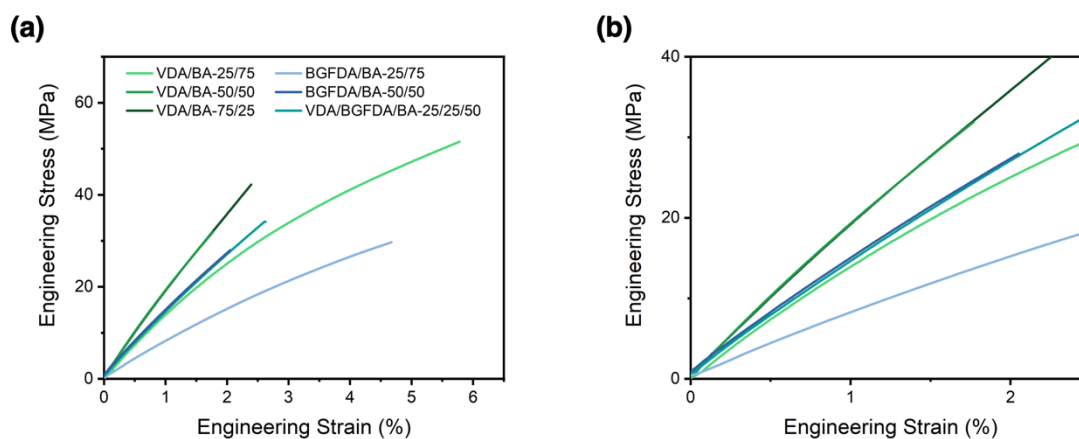


Fig. S13 Uniaxial tensile curves of acrylate networks for (a) full scale and (b) scale in the low strain region.

Table S2 Uniaxial tensile properties of acrylate networks

	E_t (GPa)	ε_B (%)	σ_M (MPa)	Toughness (MJ m ⁻³)
VDA/BA-25/75	1.3 ± 0.1	4.3 ± 1.6	40.6 ± 6.3	1.1 ± 0.5
VDA/BA-50/50	2.0 ± 0.4	1.6 ± 0.3	28.8 ± 4.0	0.3 ± 0.1
VDA/BA-75/25	2.0 ± 0.8	1.9 ± 0.4	32.6 ± 5.8	0.3 ± 0.1
BGFDA/BA-25/75	0.8 ± 0.2	4.4 ± 0.2	28.6 ± 1.2	0.7 ± 0.1
BGFDA/BA-50/50	1.5 ± 0.1	1.8 ± 0.3	25.4 ± 1.5	0.3 ± 0.1
VDA/BGFDA/BA- 25/25/50	1.4 ± 0.1	2.3 ± 0.3	30.7 ± 3.3	0.4 ± 0.1